

Case study: Reliquary box : Coffret-écrin de la couronne-reliquaire de la couronne-reliquaire des saintes Epines, XIIIth century, Namur (inv. n°7)

Case study image:



Authors of the report: Marina Van Bos, Ina Vanden Berghe, Maaïke Vandorpe (Labs KIK-IRPA)

Report date: 27/10/2021

1. Non-invasive analysis

1.1. Methodology

Hirox-images

Some detailed images were taken with the Hirox digital microscope (KH-8700).

MA-XRF

For the material-technical analyses X-ray fluorescence (XRF) analyses were performed. Despite a number of limitations and drawbacks, mobile XRF has been successfully used in the past for the identification of pigments in murals, manuscripts, etc.

XRF is an elemental analysis technique that makes it possible to identify the chemical elements present within the irradiated zone, without taking into account the stratigraphy. The chemical elements can thus be present both in the surface layer and / or in the underlying layer(s) (this depends on the nature of the chemical elements and the thickness of the layers).

A second disadvantage of the technique is that the information obtained is “elementary” information and not molecular information. For example, when lead is detected in a paint layer, this may indicate the white pigment lead white [$2 \text{PbCO}_3 \cdot \text{Pb}(\text{OH})_2$], or the red lead red (minium) [$2\text{PbO} \cdot \text{PbO}_2$], or the yellow massicot [PbO], or a mixture.

Light chemical elements are not detected and organic compounds cannot be identified.

This technique thus provides a general overview of the chemical elements present in the analysed zone.

The XRF technique is based on the following principle: a primary x-ray (coming from the x-ray source in the equipment) is aimed at the surface layer to be analysed. Secondary X-rays, characteristic of the chemical elements present, are generated. Due to the high energy of the incident primary x-rays, secondary x-rays are generated not only in the surface layer but also in the underlying layer(s). This obviously complicates the interpretation of measurement results.

For the investigation of some of the metal threads and the enamels on the lid of the box, we used a new way of performing XRF analyses: macro-XRF (MA-XRF, see figure 1). With this technique, a whole surface is scanned (not a point analysis) and the detected chemical elements are visualized in distribution maps. Results can only be interpreted qualitatively (no quantification of results).

The MA-XRF analyses are performed with the M6 Jetstream macro-XRF instrument, developed by the Bruker company. The measuring head moves 1 to 2 cm above the surface of the box by means of a motorized XY stage. The measuring head consists of a microfocus X-ray tube with Rh-target (30 W, voltage 50 kV, current 600 μ A).

Measurements were taken with a beam diameter of 150 μ m, 125 μ m distance between two measurement points and 40 ms measurement time per point (metal treads) and 30 ms measurement time per point (enamels). The data were collected and examined with the software of Bruker M6 Jetstream (sum spectrum and maximum pixel intensity spectrum).

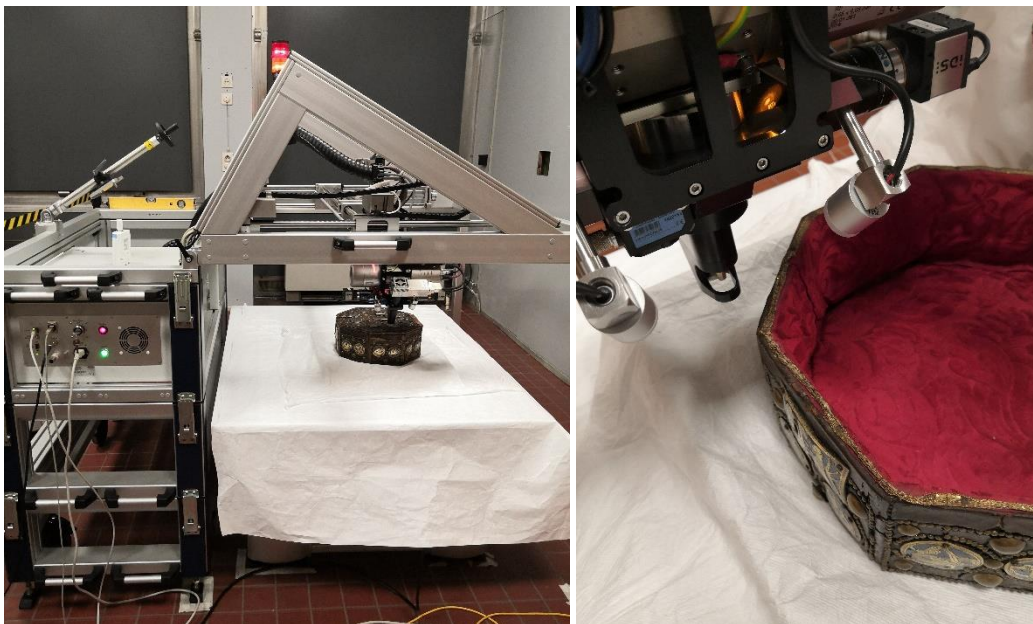


Figure 1: MA-XRF equipment

The distribution plots are 'grey scale maps': black corresponds to the absence of the element, white means that the element is abundant present and the different grey values correspond to intermediate 'quantities'.

1.2. Results

1.2.1. Metal threads

The two zones analysed by MA-XRF are indicated in figure 2, the results of the 2 scanings are summarized in figure 3 and 4.



Figure 2: indication of the 2 zones analyzed by MA-XRF (image before textile conservation, analyses after textile conservation)

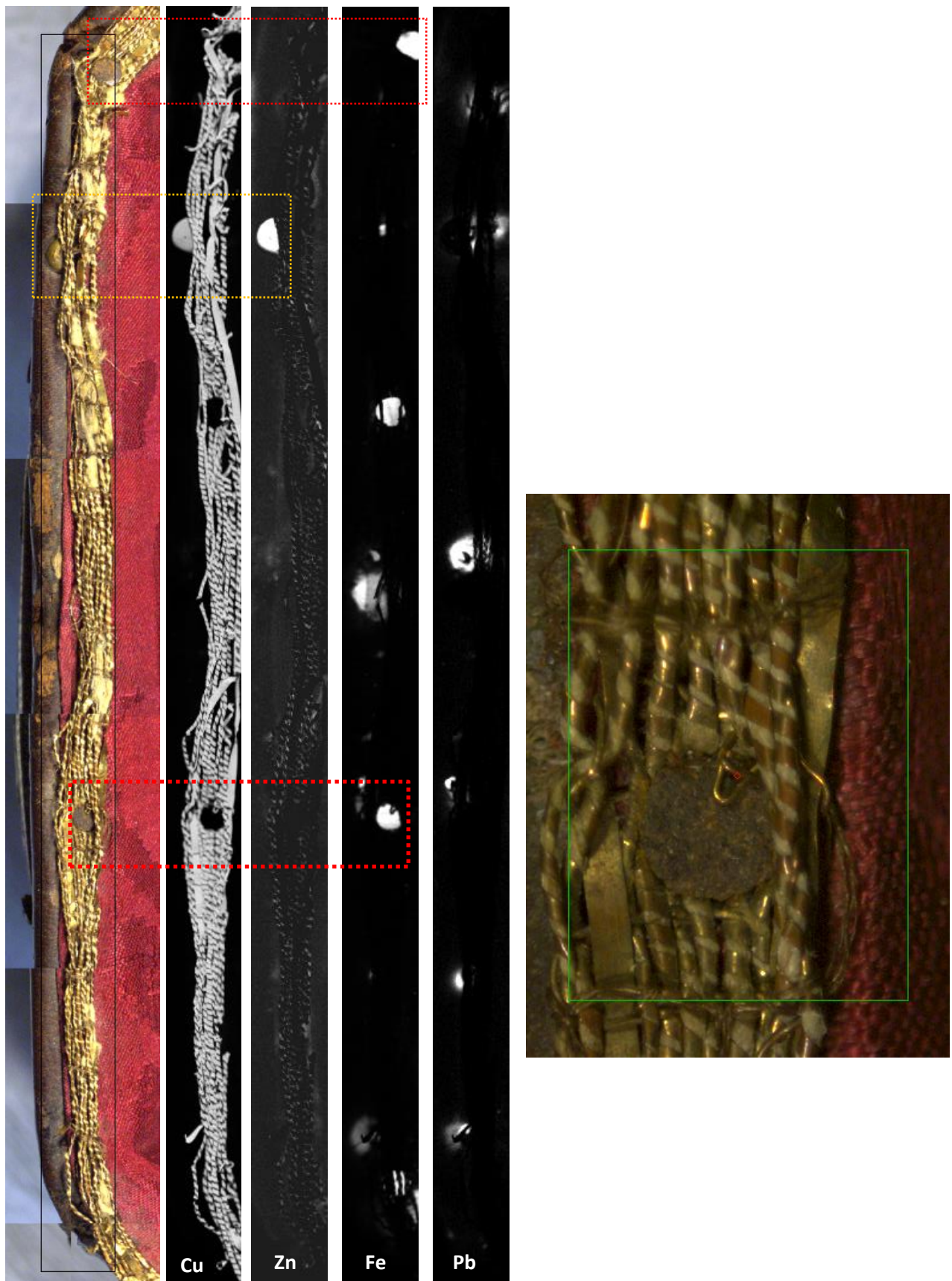


Figure 3: composed image (M6 camera) of the analyzed area 1 with distribution map of copper (Cu), zinc (Zn), iron (Fe) and lead (Pb) and detailed image (M6 camera) (from left to right)

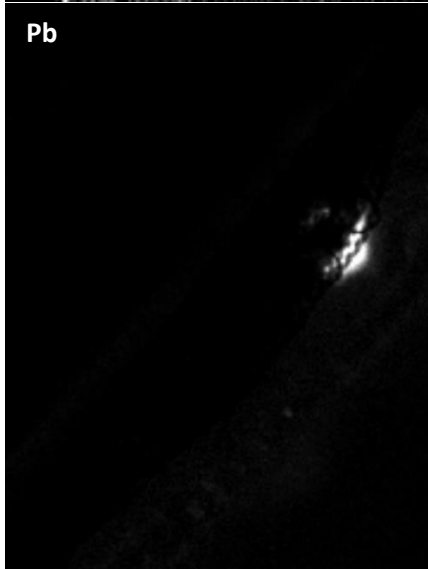
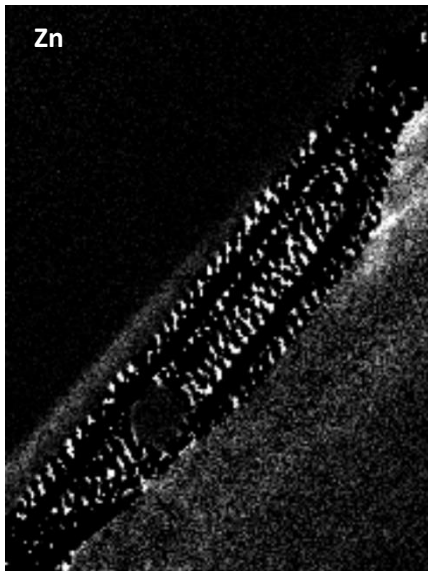
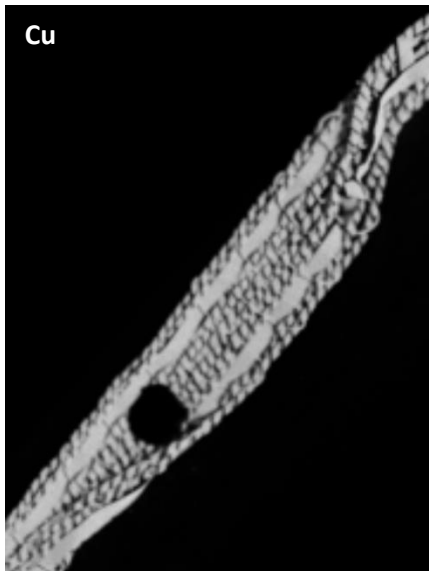
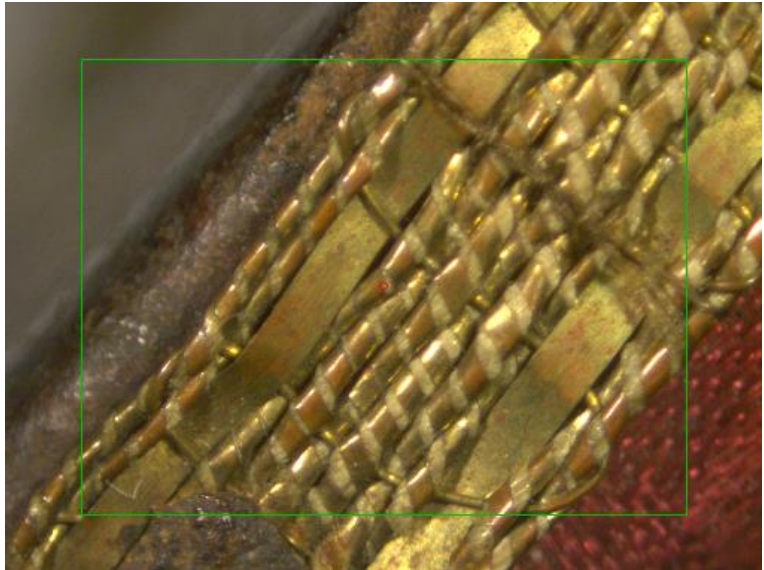
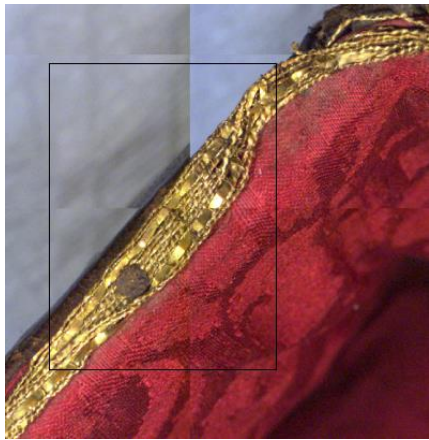


Figure 4: composed image and detailed image (M6 camera) of the analyzed area 2 with distribution map of copper (Cu), zinc (Zn), iron (Fe) and lead (Pb)

On the inside of the box, metal threads are present, either as thread wrapped around a textile thread, either as flat lamella.

The wrapped metal thread is clearly composed of copper (Cu) and zinc (Zn), indicating the alloy brass.

The flat lamella is composed of copper with very minor amounts of zinc (almost not visible in the distribution maps of figure 3 or 4).

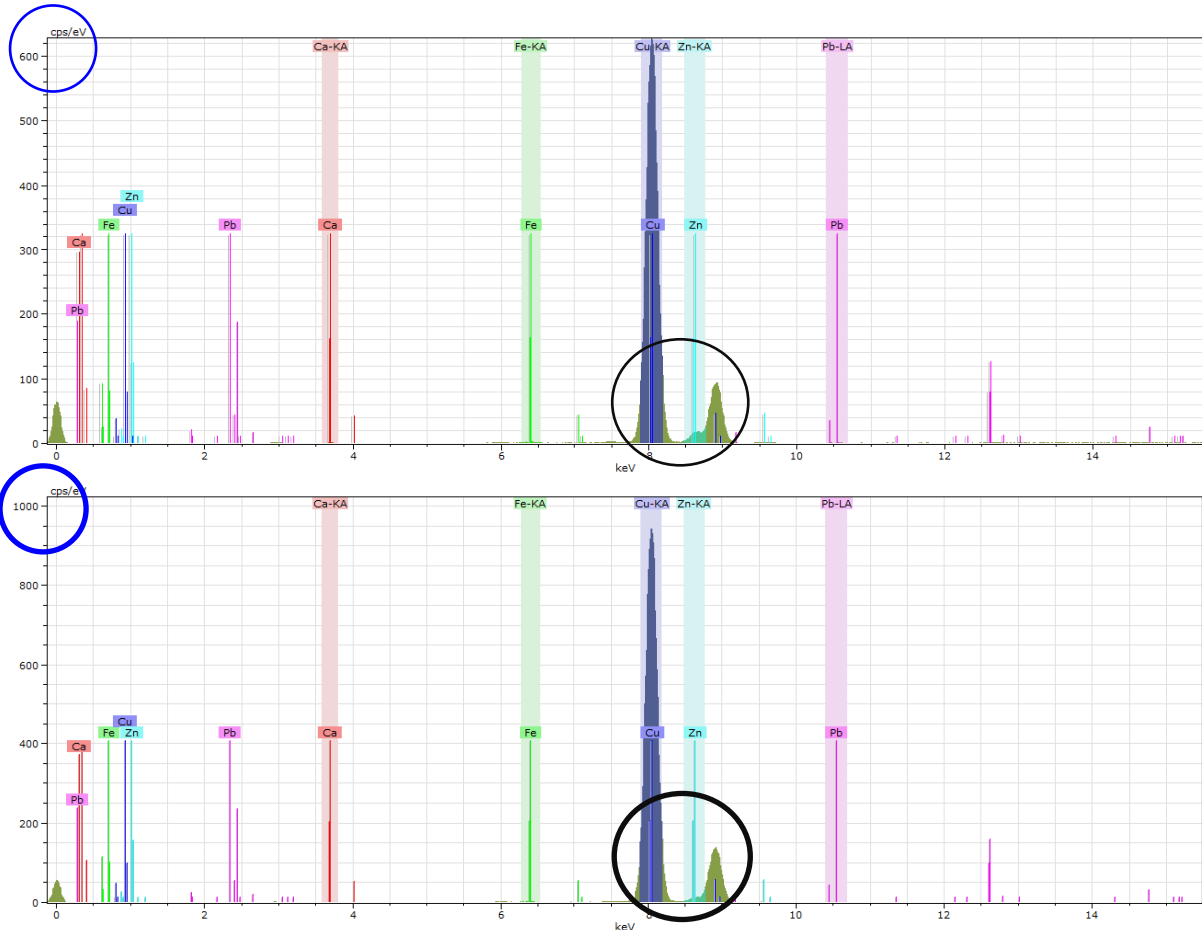


Figure 5: XRF spectrum of the wrapped metal thread (top) and of the flat lamella (bottom)

The different copper/zinc ratio for the wrapped thread and the flat lamella is also reflected in a color difference as shown by the Hirox images in figure 6 and 7. This color difference (and hence a composition difference?) is not observed everywhere (see figure 8).

The distribution plot of copper and zinc in figure 3 show also very clearly the presence of a brass nail head (see orange rectangle in figure 3 and figure 7), the distribution plot of iron corresponds to the presence of iron nails (see red rectangles in figure 3 and figure 6).

The presence of lead corresponds to some internal parts of the box (nails, solder,...) which are not visible.



Figure 6: Hirox image showing some of the metal threads inside the box (different color for the wrapped thread or the flat lamella) and an iron nail head



Figure 7: Hirox image showing some of the metal threads inside the box (different color for the wrapped thread or the flat lamella) and a nail head in brass



Figure 8: Hirox image showing some of the metal threads inside the box (no clear color difference between the wrapped thread or the flat lamella).

1.2.2. Enamel medallions

Results are presented as distribution maps of the different detected chemical elements per analysed enamel (see figure 9 for the enamel numbering). Because light chemical elements are not detected by MA-XRF, it's not possible to characterize the glass components. The results will be interpreted in terms of the added metal oxides.

The following abbreviations for chemical elements are used:

As: arsenic
Au: gold
Ca: calcium
Co: cobalt
Cu: copper
Fe: iron
Hg: mercury
Mn: manganese
Pb: lead
Sb: antimony
Sn: tin
Zn: zinc

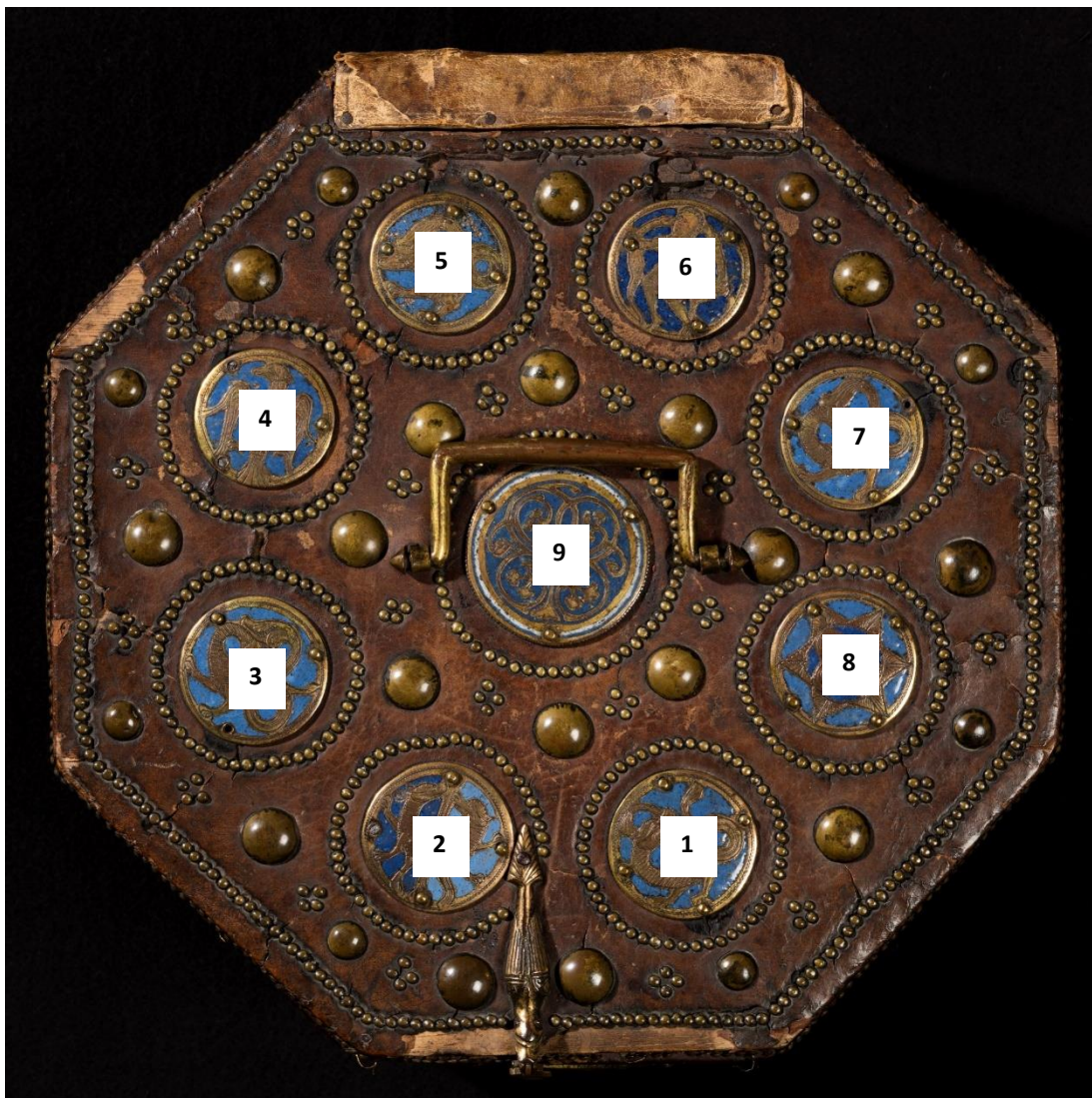


Figure 9: analyzed enameled medallions

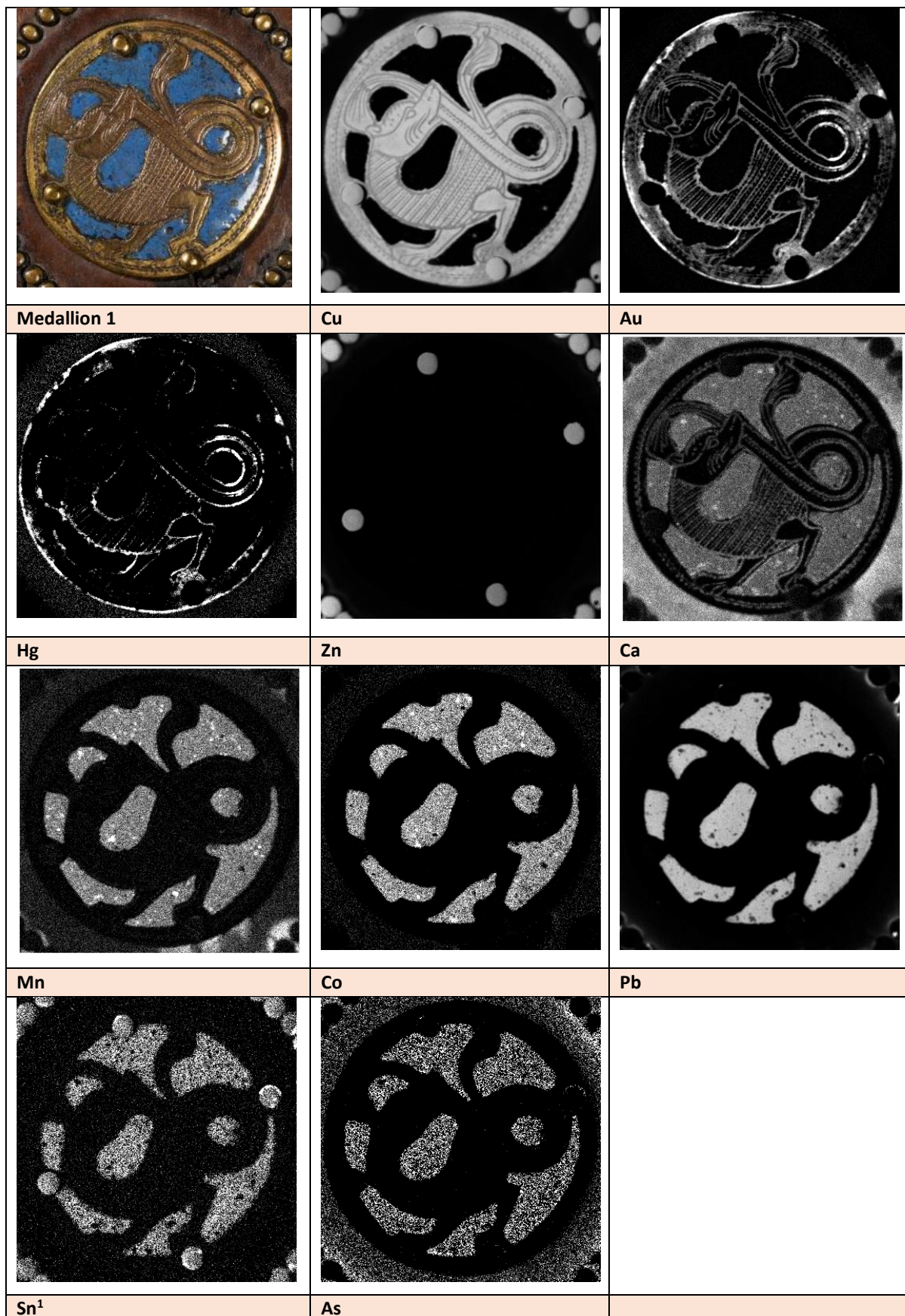


Figure 10: MA-XRF analysis results of medallion 1

¹ The following X-ray lines are used to draw the maps: $K\alpha$ lines of Ca, Mn, Fe, Co, Cu, Zn, Sn, Sb; $L\alpha$ lines of Hg, Au, Pb; $K\beta$ line of As

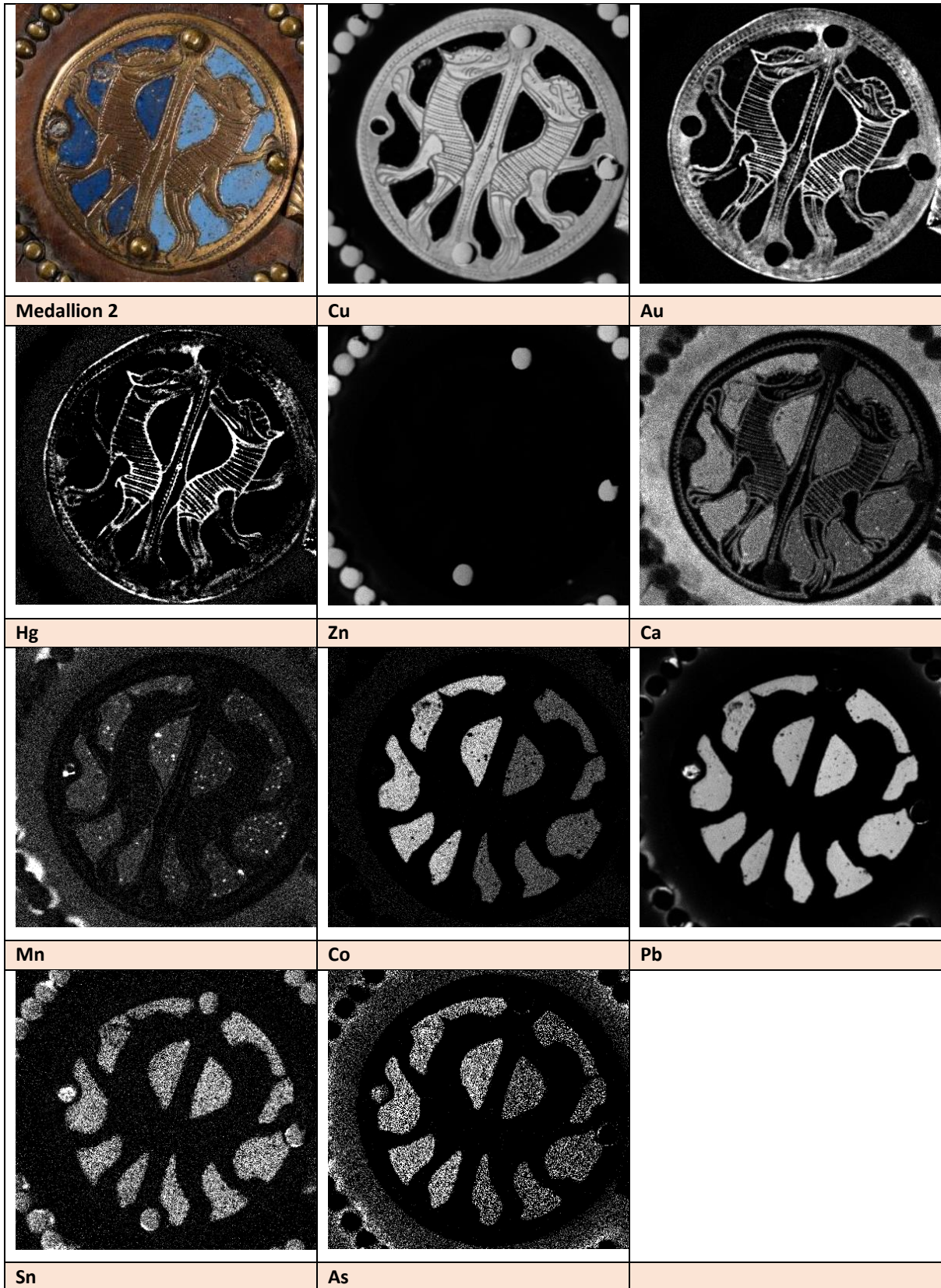


Figure 11: MA-XRF analysis results of medallion 2

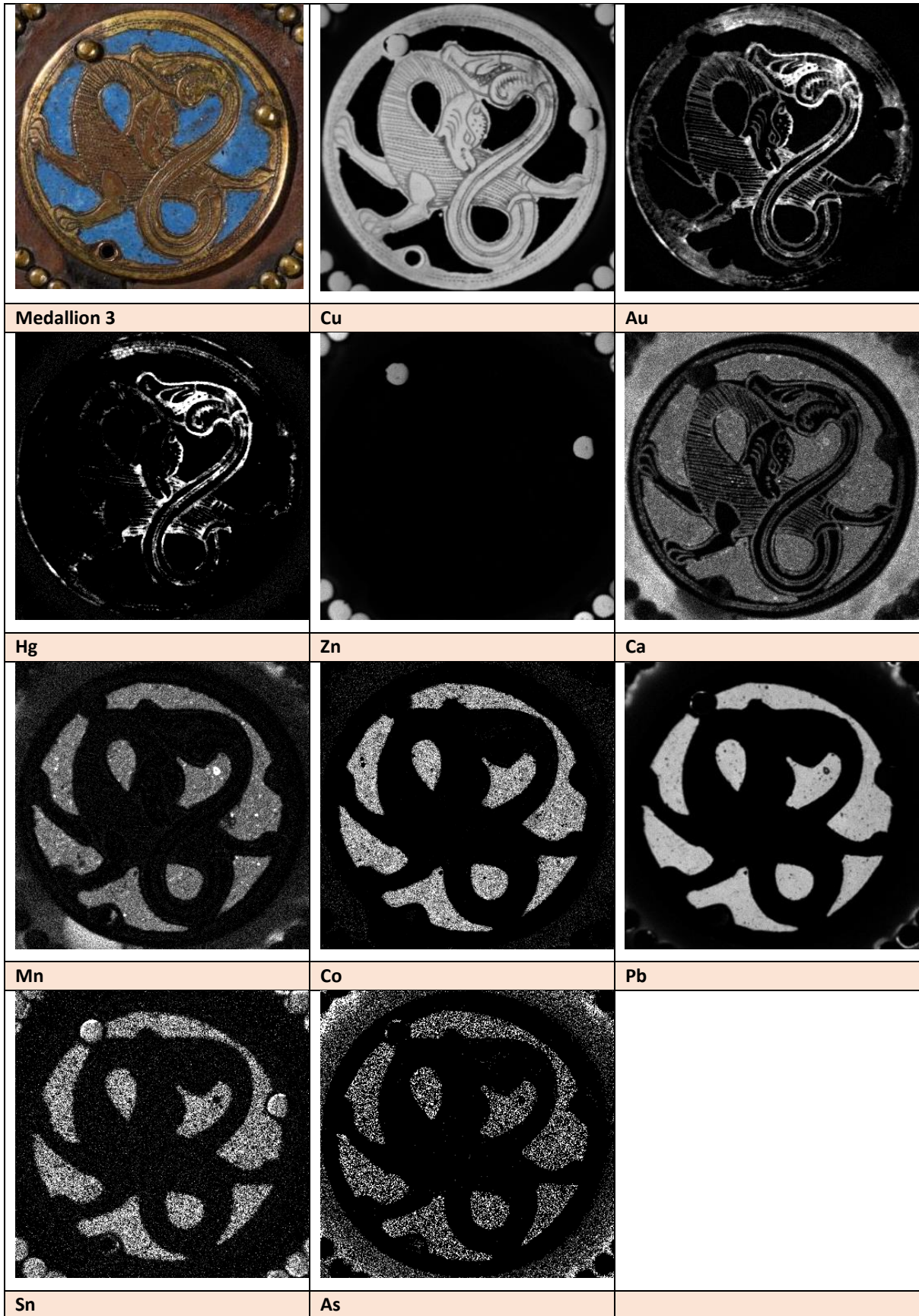


Figure 12: MA-XRF analysis results of medallion 3

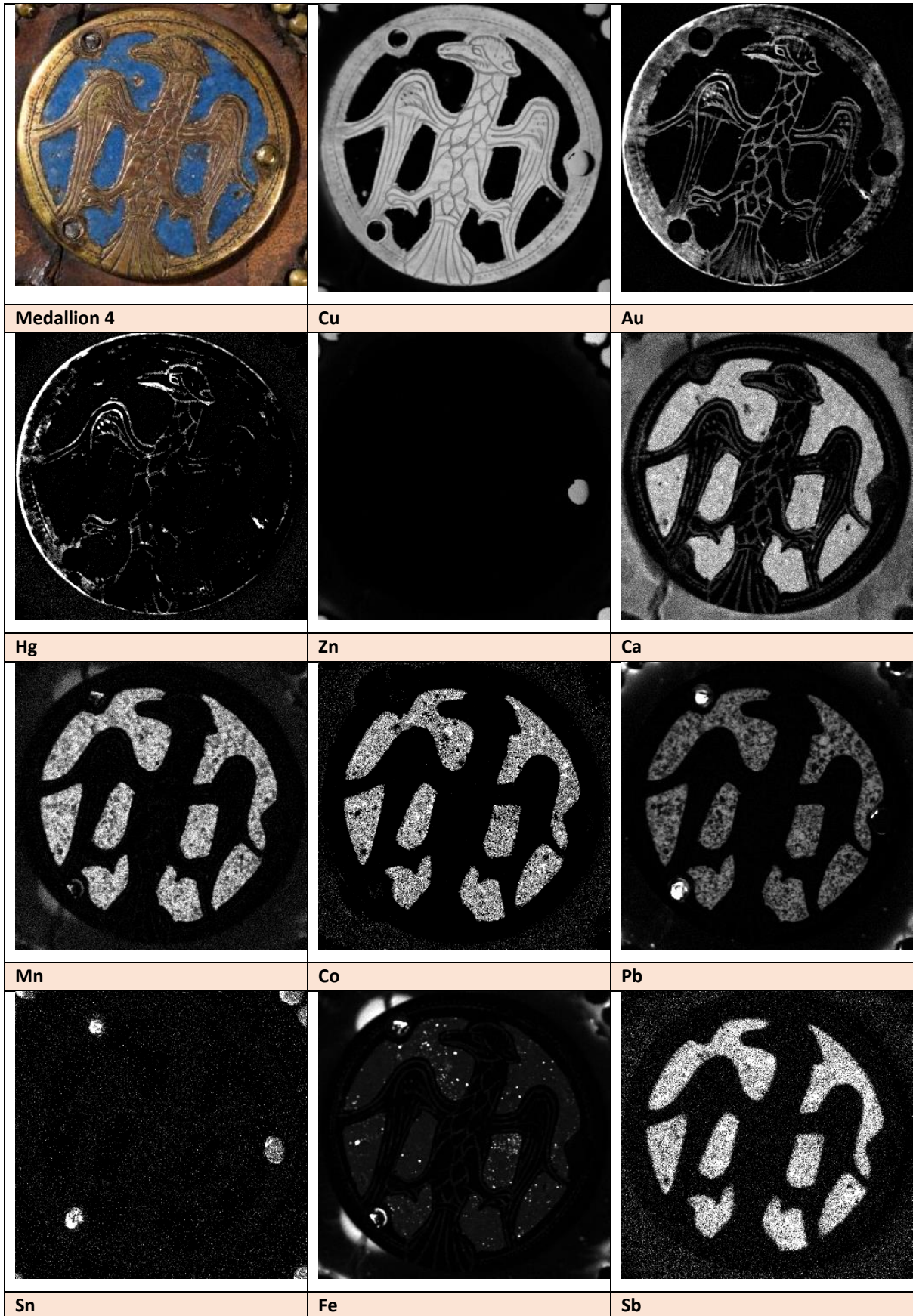


Figure 13: MA-XRF analysis results of medallion 4

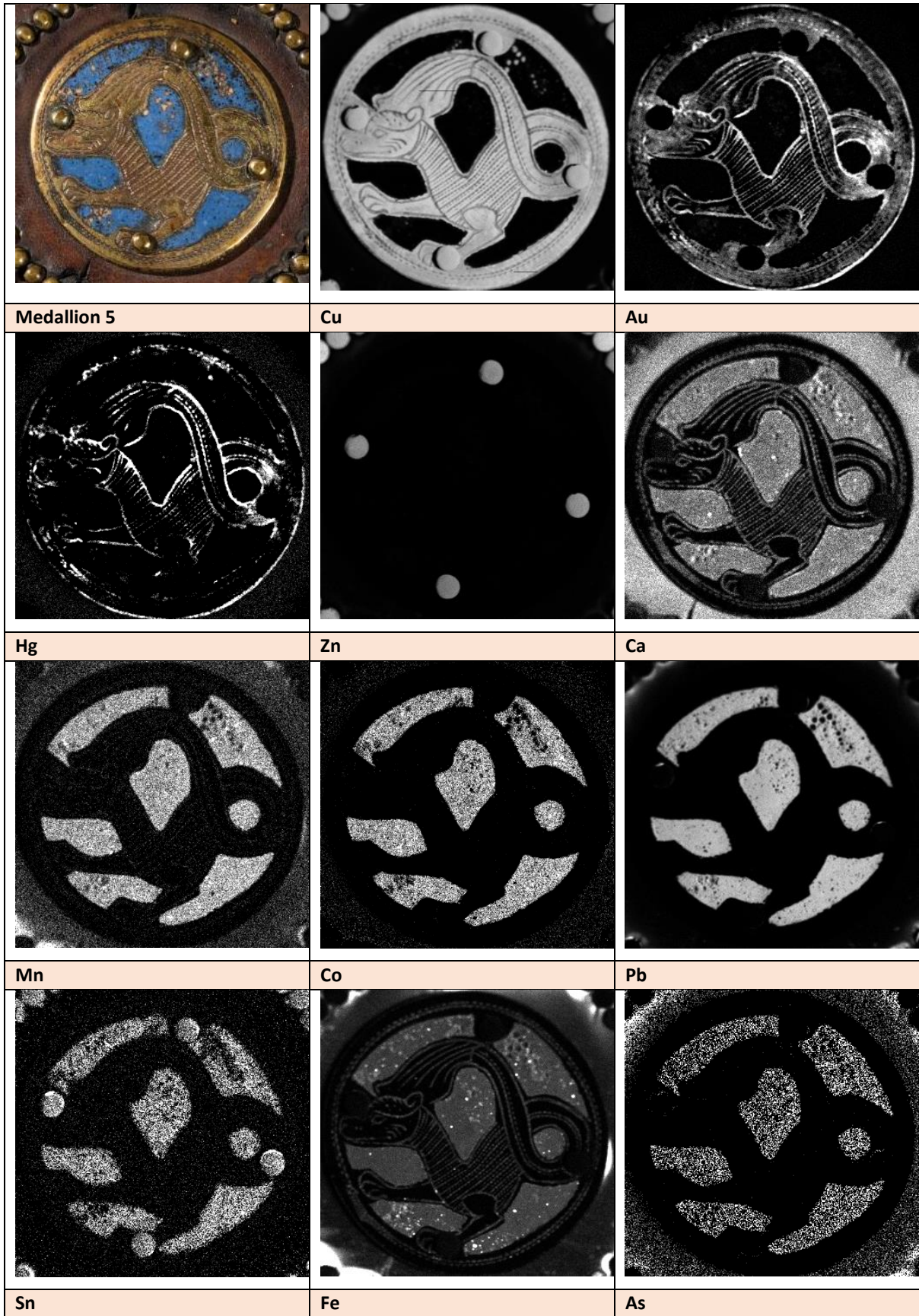


Figure 14: MA-XRF analysis results of medallion 5

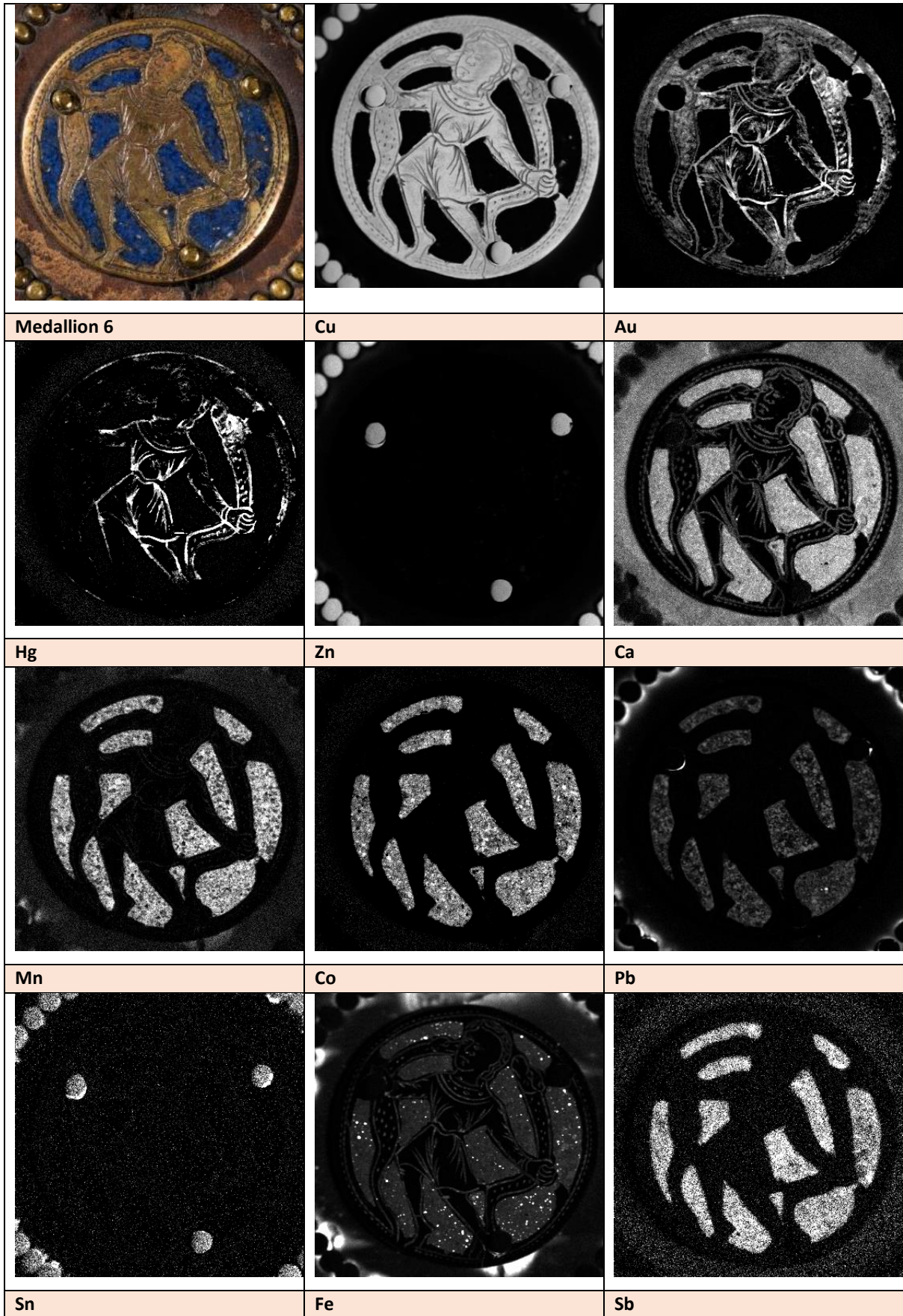


Figure 15: MA-XRF analysis results of medallion 6

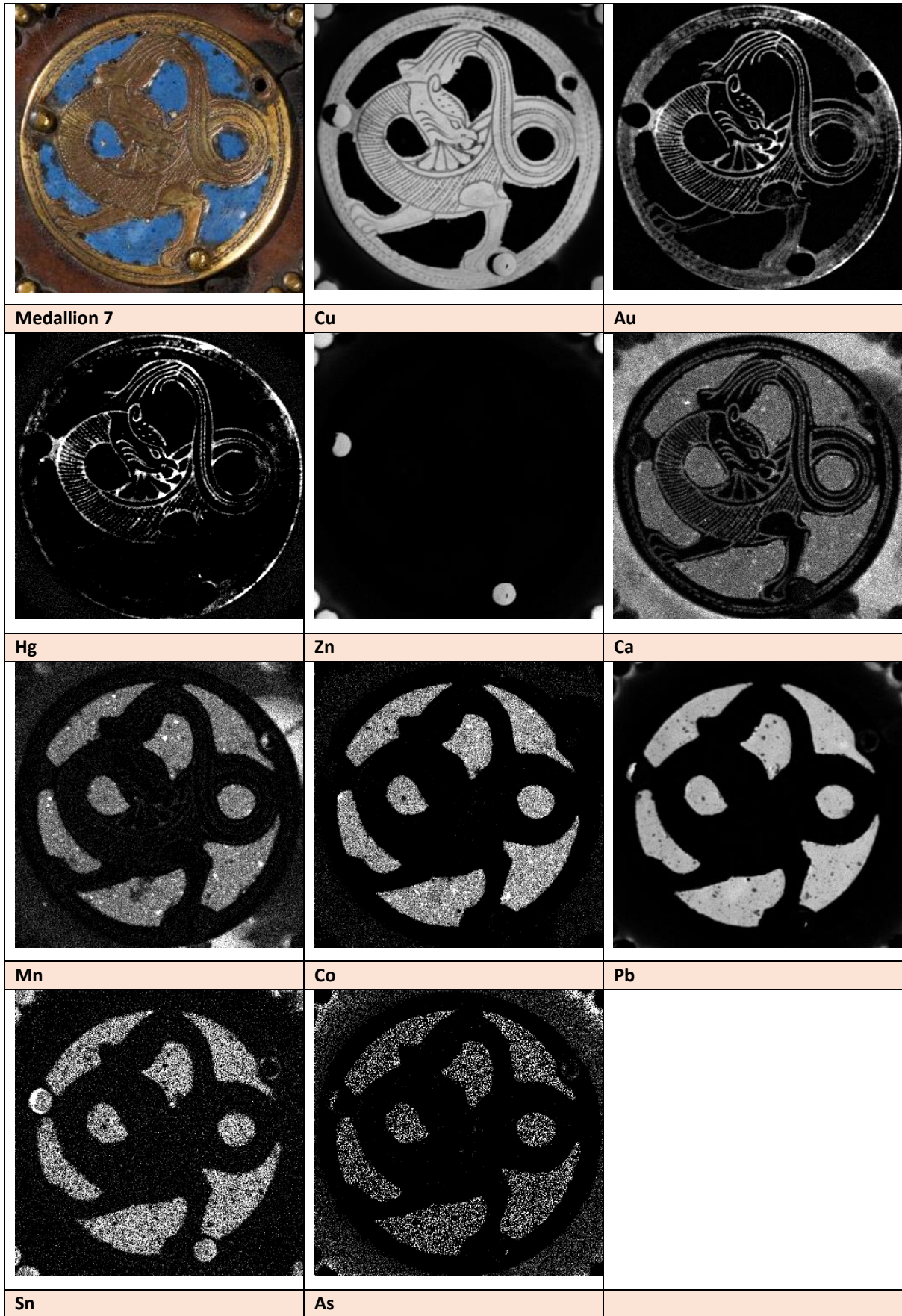


Figure 16: MA-XRF analysis results of medallion 7

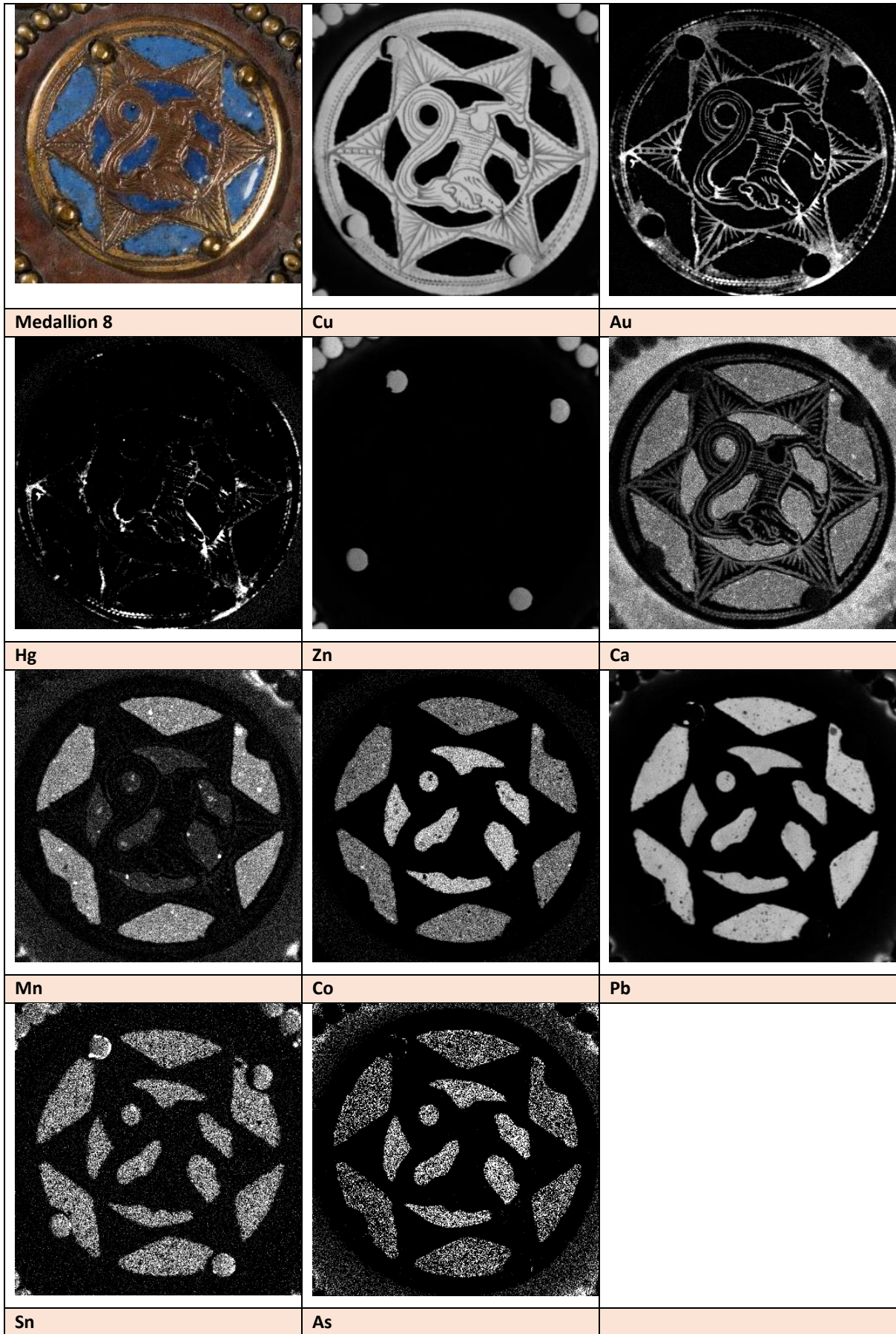


Figure 17: MA-XRF analysis results of medallion 8

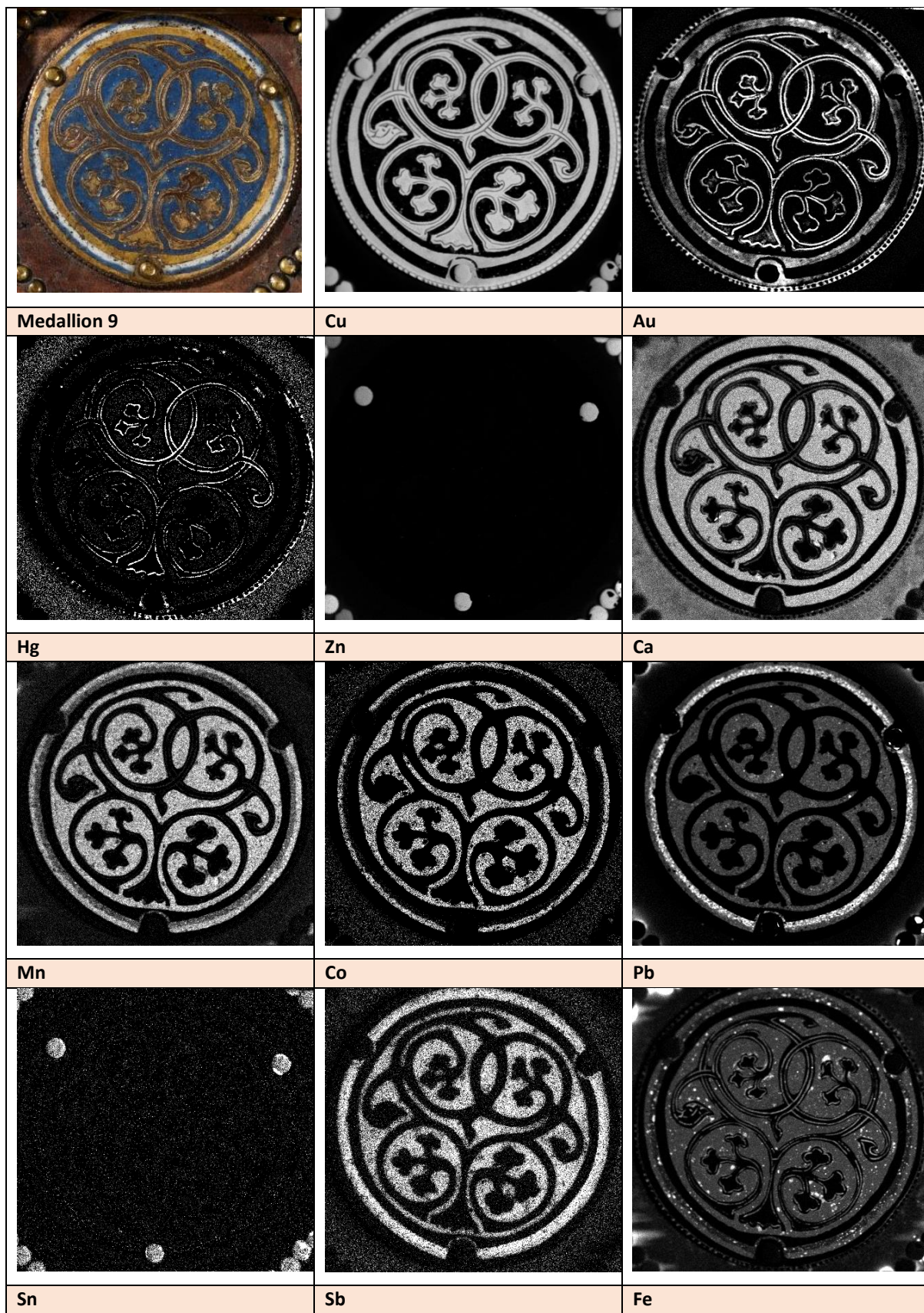


Figure 18: MA-XRF analysis results of medallion 9

Champlevé is an enameling technique in which, depending on the design of the décor, cavities are made in the metal support and filled with vitreous enamel. The piece is then fired until the enamel fuses, and when cooled the surface of the object is polished. The uncarved portions of the original surface remain visible as a frame for the enamel designs, typically they are gilded.

Enamel is a mixture of silica, lead, potash and soda. By melting these different components at high temperature, after grinding, a colorless powder is obtained, called a "flux". This "flux" is colored by adding metal oxides. This mixture is deposited on a metal support. The art of the enameller consists in fixing the enamel powder on its metal support by successive short fires of the order of 800 degrees.²

The metal support

The metal support is a gilded copper plate (see figure 19 and maps of gold (Au) and copper (Cu) in figures 10-18), the gold being applied by 'amalgam gilding' (= a gold gilding technique in which an amalgam of Gold with Mercury is applied to a metal, such as copper or silver, then the metal is heated to flash volatilize the mercury and deposit a thin layer of gold) (see figure 19 and maps of mercury (Hg) in figures 10-18).



Figure 19: false color images; left: distribution of copper (in yellow) and gold (in red) for medallion 2; right: distribution of gold (in yellow) and mercury (in red) for medallion 8

The presence of a thin gold layer is less evidenced on some parts of some medallions, probably as a result of wear (see figure 20).

² "Enamels of Limoges. 1100-1350", The Metropolitan Museum of art, N.Y., J.P. O'Neill (Ed), 1996



Figure 20: Hirox images showing details of medallion 2 (above), medallion 5 (middle, enamel surfaces show pitting corrosion) or medallion 6 (bottom): some parts of the copper have a more yellowish color (presence of gold) compared to other parts.

As specified in some medieval treatises (like Theophilus's *De Diversis Artibus*) the used copper has a high level of purity ($\geq 98\%$).

The metal nails

Together with the enamels, both the nails used to fix the copper plates onto the box and some of the nails used as circular decoration around the enamel medallions were analyzed (in fact: not the nails themselves but the decorative rounded heads of the nails).

As evidenced by the distribution maps of copper and zinc, the nail heads are composed of brass, an alloy of copper and zinc (see figure 21 and maps of zinc (Zn) and copper (Cu) in figures 10-18).



Figure 21: false color image: distribution of copper (in yellow) and zinc (in blue) for medallion 6

On medallion 2, one nail head is missing; on medallion 4, two nail heads are missing. In these areas, lead and tin can easily be detected.



Figure 22: detail of medallion 2 with the missing nail head and false color image showing the distribution of lead (in white) and tin (in purple).

The co-presence of lead and tin can easily be observed when the nail head is missing (see figure 22).

When the nail head is present, the presence of tin is still clearly visualized in the distribution maps (see figures 10-18); lead can only be seen on the edges, where the solder comes out from under the nail head (see figure 22, areas highlighted with arrows and distribution maps of lead in figures 10-18; see also figure 23 with a detail image of medallion 9).



Figure 23: Hirox image with detail of medallion 9: the greyish solder material is visible near the nail head

The lead-tin alloy, used as solder material, was already described by Pliny the Elder³, in his *Historia Naturalis*, written 2000 years ago.

The enamels

Medieval enamels have a composition comparable to that of the Roman period: soda-lime glass, opacified with tin or antimony oxides.

In the article 'Techniques and Materials in Limoges Enamels'⁴, the composition of enamels is specified for enamels before and after the beginning of the 13th century (see table 1).

Table 1: composition of enamels (weight%), table copied from the above mentioned article

	Sodium	Magnesium	Aluminum	Silicon	Potassium	Calcium	Tin	Antimony	Lead
	Na ₂ O	MgO	Al ₂ O ₃	SiO ₂	K ₂ O	CaO	SnO ₂	Sb ₂ O ₃	PbO
Early Type:	10-20	0.2-2.0	1.5-4.5	55-70	0.5-1.5	5-10	<0.5	0.5-10	0.5-10
Late Type:	10-18	1.5-5	0.5-3.5	45-55	1.5-2.5	2-8	5-15	<0.5	5-20

Taking into account the limitations of the MA-XRF technique (see the introduction in this report), the differences which can also be observed during our MA-XRF analyses refer to the presence of tin or antimony.

³ in Chapter XLVIII of Book XXXIV, one can read that that the solder connections of the pipes of the Roman aqueducts were made with a mixture called tertiarium, an alloy of two parts lead and one part tin.

⁴ See footnote 2

Table 2 summarizes the blue enamel composition (see figures 10-18) of the reliquary box. The composition is expressed as:

- + present
- ++ present in 'more than normal' amount
- / not present
- present in only very minor amount

Table 2: composition of the blue enamels on the lid of the reliquary box

	Ca	Mn	Co	Pb	Sn	Sb
Med. 1	+	+	+	+	+	/
Med. 2 light blue	+	/	+	++	+	/
Med. 2 dark blue	++	/	++	+	+	/
Med. 3	+	+	+	+	+	/
Med. 4	++	+	+	-	/	+
Med. 5	+	+	+	+	+	/
Med. 6	++	+	+	-	/	+
Med. 7	+	+	+	+	+	/
Med. 8 light blue	+	+	+	+	+	/
Med. 8 dark blue	+	/	++	+	+	/
Med. 9	+	+	+	-	/	+

All enamels contain cobalt(oxide) as blue colorant.

Calcium antimonate and tin oxide are historically the most used opacifiers. The blue enamels on medallion 4, 6 and 9 contain antimony but no tin.

Referring to table 1, these enamels could be dated as early 13th century.

Vitreous materials, containing tin, contain very often also lead oxide because lead oxide would facilitate the conversion of metallic tin to tin oxides⁵.

Arsenic oxide, used as opacifier is typical for 19th century productions. The low 'amount' of arsenic, present in all medallions (see figures 10-18) must be seen as an impurity in the cobalt and not as a marker to 'date' the enamel⁶.

⁵ See footnote 2

⁶ João Manuel Mimoso "Origin, early history and technology of the blue pigment in azulejos" in GlazeArch 2015. International Conference Glazed Ceramics in Architectural Heritage

And N. Eastaugh, V. Walsh, T. Chaplin, R. Siddall 'Pigment Compendium. A Dictionary and Optical Microscopy of Historical Pigments', Elsevier, 2008 ('smalt', p351-352).

Both the light and the dark blue on medallion 2 and the dark blue on medallion 8 have no manganese (see figures 10-18 and figure 24).

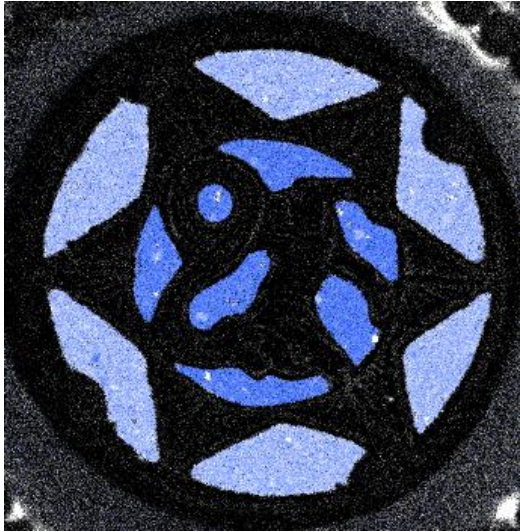


Figure 24: false color image: distribution of cobalt (in blue) and manganese (in white) for medallion 8

Because of the heat needed to fuse the enamel, red copper oxide (cuprite) was typically formed (see figure 25).

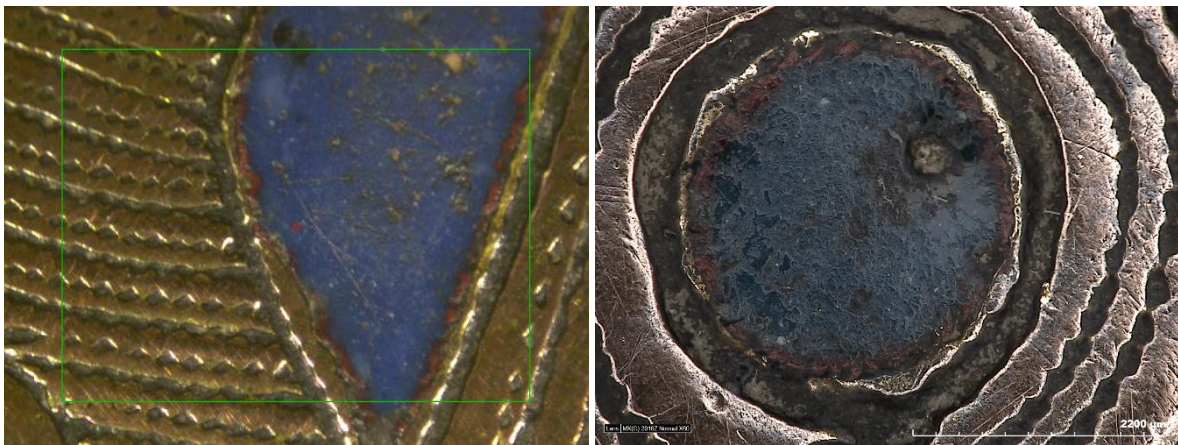


Figure 25: (left): detail of medallion 2 (image taken by the M6-camera) ; (right) detail of medallion 4 (Hirox image) showing the presence of red cuprite

1.2.3. The leather

Original leather



Figure 26 (A-B-C): Hirox images of the original leather



Figure 26 (D-E-F): Hirox images of the original leather



Figure 26 (G-H-I): Hiox images of the original leather



Figure 26 (J): Hirox image of the original leather

In figures 26 (A-D), the pattern of hair pores can easily be discerned. The hair pores are evenly distributed over the skin. This pattern looks like the pattern of cow (or calf) skins. (Cow and calf skins have the same pattern): no rows of hair in which follicles are clustered together in one direction and farther apart in another⁷.

The deterioration of the leather is illustrated in figures 26 D-J:

Figures 26 E-F show a (circular) cracking in the leather at the contact point with the nails. From there, the cracks continue.

The surface layer flakes off and the grain layer of the leather disappears; the fiber structure of the underlying leather tissue becomes visible (figures 26 G-I).

At some parts, all of the leather is missing (figure 26 J).

The deterioration is probably a result of the combined effect of mechanical damage (nails used to fix the leather and thus perforating the leather) and damage by climatological conditions (large climatic variations make the leather shrink and expand causing deformations and cracks)⁸.

⁷ www.leather-dictionary.com

and

<https://travelingscriptorium.files.wordpress.com>

blog-post-on-parchment-and-leather-identification.edited.pdf (wordpress.com)

⁸ Lieve Watteeuw : VerzekeDe Bewaring: "Leder en perkament", FARO

The restoration leather used as hinge for the lid

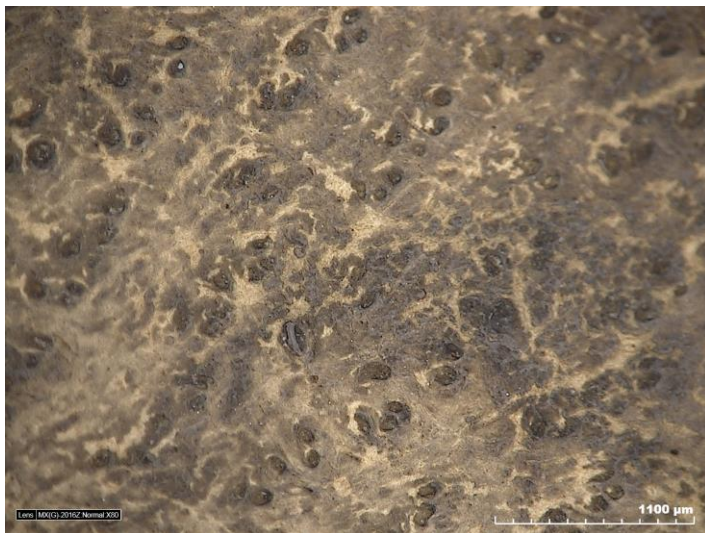


Figure 27 (A-B-C): Hirox image of the restoration leather



Figure 27 (D-E): Hirox image of the restoration leather

The hair pores (see figure 27 A-D) in the leather skin are present in different clusters, spread out in wide-set rows. This points to a sheepskin.

Part of the surface layer of this leather is already missing (deterioration of the leather).

2. Invasive analysis

2.1. Textile

Sample Description

The inner side of the box is covered by a **red damask silk fragment**, from which a thread sample was taken for dye (/k01) and fibre identification (/v01) (figure 28).



Figure 28: The reliquary box with indication of the sample location

In addition, a sample was taken from **the filling** to determine whether the filling is original or not (v/02) (detail figure 29).



Figure 29: Hirox image of the filling fibres at the area of sampling (magnification 20x)

A **small metal decoration band** is present at the border between the leather from the outside and the silk fragment at the inner side (figure 30). This decoration band is composed of both metal threads with a textile core and a metal lamella, from which as sample of each was taken, respectively (/m03 and /m04).

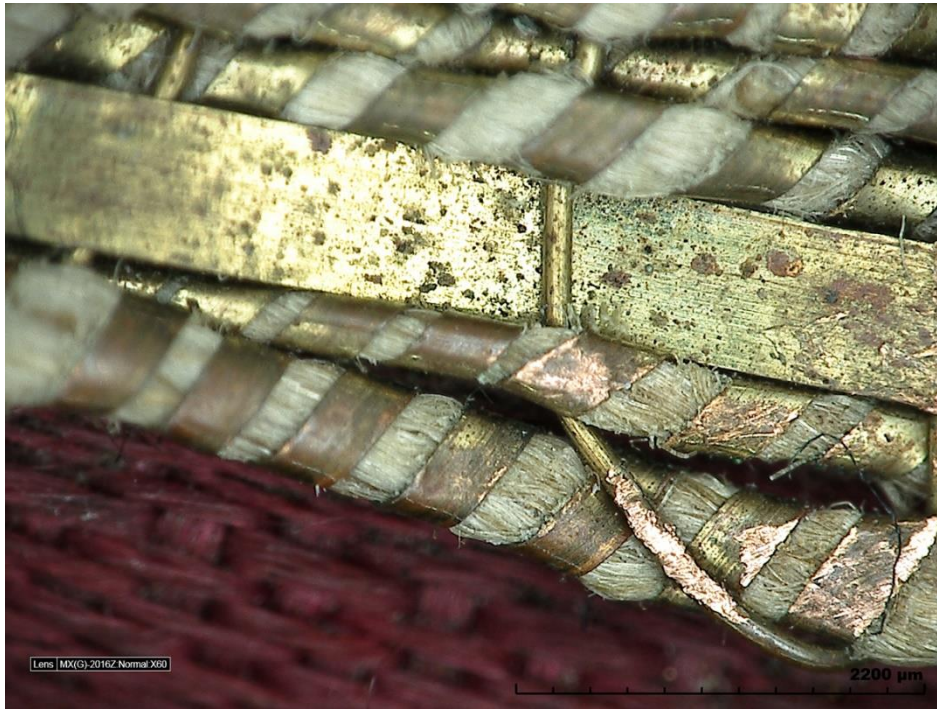


Figure 30: Detailed Hirox image of the metal decoration band (magnification 60x)

The dyes used for the red damask from the reliquary box are compared to the dyes used in a **similar damask weave fragment currently present at the Diocesan Museum of Namur** (figure 31). The textile measures 46 x 37 cm. It is hemmed and may have been used as an altar cloth. Another similar red damask weave is the textile from figure 32, a cope from the Saint-Aubain Cathedral (no inv. number nor KIK number).

As it might be possible that the first fabric has been used for the re-lining of the box at the end of the 19th century, a sample of that red silk was sent to the textile lab by H el ene Cambier, conservator of the Treasure of the Cathedral and Diocesan Museum (sample /k05).



Figure 31: red silk damask fragment from the Diocesan Museum of Namen (sample /k05)

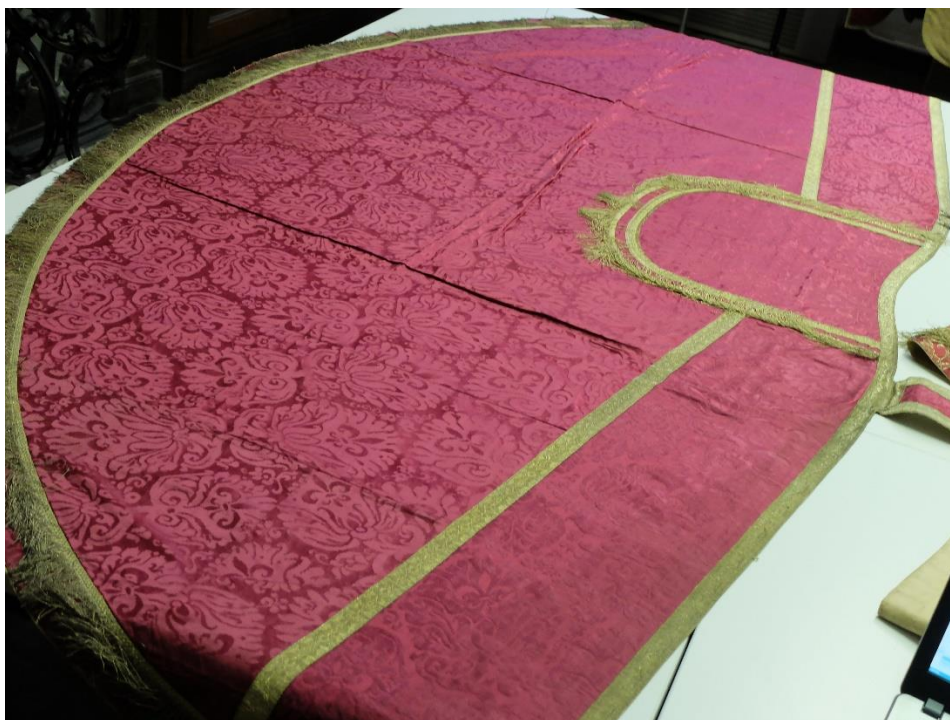


Figure 32: Cope made of 'similar' red silk damask from the Saint-Aubain Cathedral

Table 3: Overview of the samples with indication of the object, sample description and image and the KIK sample code and type of analyses

Object	Sample description	Image + KIK/IRPA code (images©KIK-IRPA Textile Lab)	Analysis / Technique(s)
Red damask weaving	Red silk	 <p>13621/k01</p>	Dye identification (HPLC-DAD)
	Red silk	<p>13621/v01</p>	Silk degradation (HPLC-FL; FT-IR, MRS)
Filling	White fibres	 <p>13621/v02</p>	Fibre identification (OM)
Metal yarns	Metal thread with textile core	 <p>13621/m03</p>	Identification of the composition of the metal thread (SEM-EDX, OM)

	Metal lamella	 13621/m04	Identification of the metal (SEM-EDX)
Damask from the museum of Namen	Red silk	 13621/k05	Dye identification (HPLC-DAD)

2.1.1. Methodology

HPLC-DAD

The identification of the organic colorants is performed by High Performance Liquid Chromatography and photo diode array detection system (HPLC-DAD) with Alliance HPLC equipment (Waters, USA). The analyses are interpreted using the Empower software system from Waters. A detailed description of the analytical protocol was published before (Vanden Berghe et al. 2009). The colorants are recovered from the fibres using acidic extraction with hydrochloric acid (HCl)⁹. Hydrochloric acid extraction was preferred to extract the dyes, as to identify a very wide range of organic dyes, either natural or (half) synthetic, by comparison with spectra from the in-house developed textile colorant reference database. Preliminary to the analysis, the samples are examined under binocular in order to avoid any visible surface contamination.

The result of the HPLC-DAD analyses are listed in Table 2. The first column comprises the code of the sample given by KIK-IRPA, followed by the sample colour in the next column. The type of extract analysed and the analysis code are mentioned in the third and fourth columns. The results of the chromatographic analyses are given in the following two columns. The dye composition mentioned in column five is expressed as relative proportions of the dye constituents after calculation of their peak area measured at the wavelength (nm) mentioned in column six.

⁹ Extraction in 250 μ L water/methanol/37% HCl (1/1/2, v/v/v) for 10 minutes at 105°C - vacuum evaporation - dissolving the residue in 30/30 μ L methanol/water from which 20 μ L is injected

Fibre

Fibre identification is carried out with optical microscopy under transmitted or polarizing illumination (OM, AxioImager M1, Zeiss). For this, a few fibres are taken from each sample. Prior to the analysis, the sample is examined under reflective light using the digital microscope KH 8700 from Hirox.

The identification of the fibres is carried out on the basis of the fibre morphology in longitudinal view. Vegetable fibres are identified by their diameter and the presence of characteristic properties (1967; Von Bergen and Krauss 1945). Animal fibres are characterized on the basis of their diameter, the presence of a cuticle with specification of the scales, the cortex (pigmented or not) and the presence or absence of a medulla and the type (Petraco and Kubic 2004). If relevant, the medullary index is also determined, based on which a distinction can be made between hair of animal and human origin (Kshirsagar et al. 2009).

The morphology of the fibres is then compared with that of reference fibres derived from published atlases (1967; Von Bergen and Krauss, 1945), online atlases and / or the internal KIK database (Vanden Berghe).

Identification between the different bast fibres is based on their differences in fibrillar orientation. This test is known as the modified Herzog or red plate test (Petraco & Kubic 2004; Haugan 2013).

Metal threads

The characterisation of the composition of a metal thread starts with a macroscopic examination of the morphology of the yarn as a whole, after which the metal strip is separated from the textile core and both are further examined separately. In the case of a metal lamella, the first step can be skipped.

If present, the fibres of the textile core are identified as earlier described in 3.2. If the textile core is coloured, the organic dyes are identified according to the procedure mentioned in 3.1.

The elemental composition of metal is studied by SEM-EDX (scanning electron microscopy coupled with energy dispersion X-ray spectroscopy, Zeiss EVO LS15 and detector of Oxford Instruments). The secondary electron images of the samples with indication of the analysed zones, as well as the corresponding spectra are shown in the added figures.

2.1.2. Results

The red silk

Carminic acid is the main dye compound detected in the two crimson red silk samples. This anthraquinone dye constituent refers to the use of the scale insect cochineal. Recalculation of the detected compounds results in the identification of the **Mexican cochineal species** (*Dactylopius coccus* Costa) (Vanden Berghe, 2016). This species was imported from the Americas since the 16th century and well-known for crimson red dyeing of silk ever since (Cardon 2007). Furthermore, tannins were used as weighting and mordant agent.

The red silk yarns used in the fabric of the reliquary box have the same dye composition of the yarns from the fragment from the Diocesan Museum, which indicate that a part of the latter textile might indeed have been used for the re-lining of the box.

Table 4. Result HPLC-DAD analyses. Detected dye composition

KIK code	Colour	Extr	Analysis n°	Dye composition	λ (nm)
13621/k01	Red	HCl	02/210208/17	2 phb, 2 mphb, + flavokermesic -C-glycoside, 42 carminic acid, 50 ellagic acid, 1 carminic acid', + carminic acid'', 1 flavokermesic acid, + kermesic acid	255
				1 flavokermesic -C-glycoside, 97 carminic acid, 2 flavokermesic acid + kermesic acid	R275
13621/k05	Red	HCl	02/210208/18	0 flavokermesic -C-glycoside, 40 carminic acid, 59 ellagic acid, 1 flavokermesic acid	255
				1 flavokermesic -C-glycoside, 98 carminic acid, 1 flavokermesic acid + kermesic acid	R275

The filling

Bast fibres were identified as the filling material. The modified Herzog test shows an fibre-orientation in S direction which indicates the use of flax (*Linum usitatissimum* L.) (Figure 33).

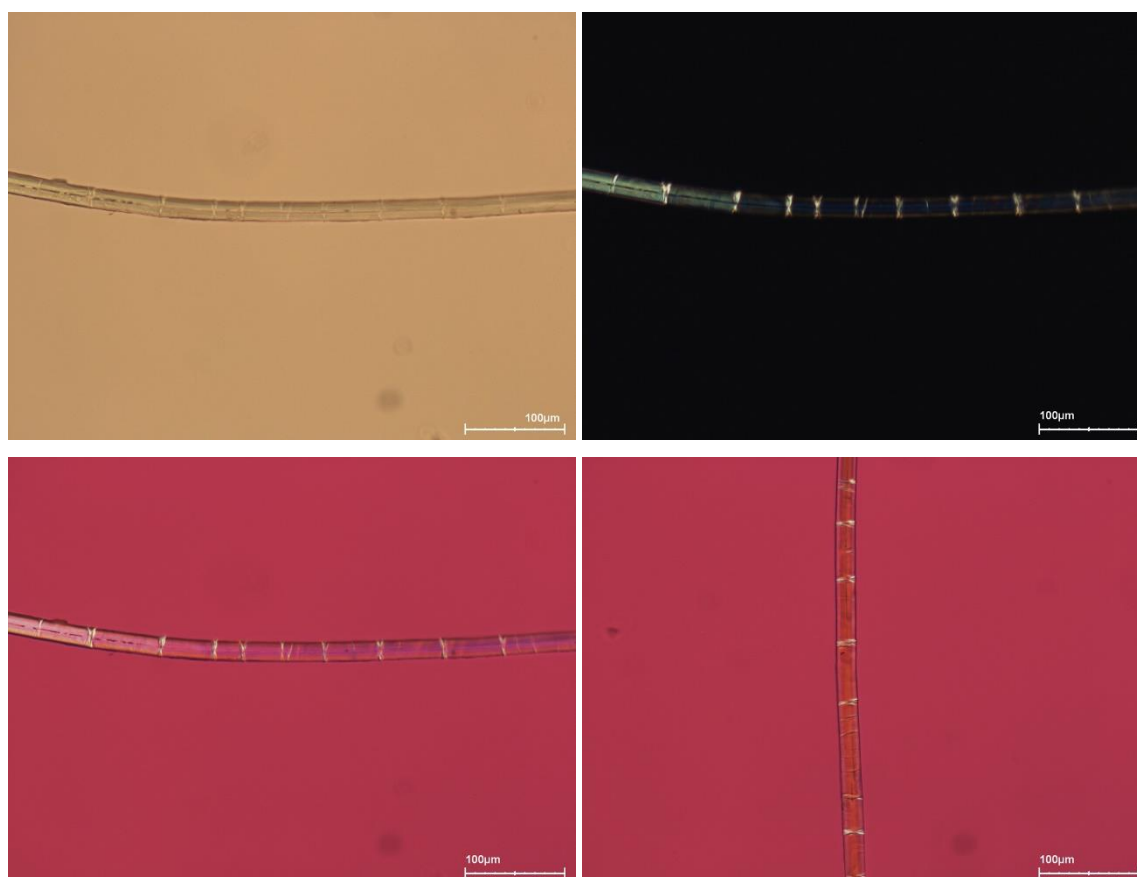


Figure 33: (top) microscopic images of sample 13621/v01 under transmitted light (left) and with the use of the polarisation filter (right) (magnification 200x); (bottom) red plate test images, the sample is blue in horizontal direction (left) and yellow in vertical direction (right) (magnification 200x)

The metal threads

The metal thread with textile core (sample /m03) is made of a metal strip wound in S-direction around a white textile core yarn. The fibres from that core yarn are identified as bast fibres. The modified Herzog test shows an fibre-orientation in S direction, which indicates the use of flax (*Linum usitatissimum* L.) (Figure 35).

The SEM-EDX analysis shows that the metal is made of brass, an alloy of copper (Cu) and zinc (Zn) in a relative ratio of 83/17 at the inside, and 86/14 at the outer surface (weight %). No traces of gold were found. The detection of chlorine (Cl), mainly on the inside, and sulfur (S) indicates the presence of corrosion of copper (figure 36-37).



Figure 34: Hirox image of sample 13621/m03 (magnification 40x)

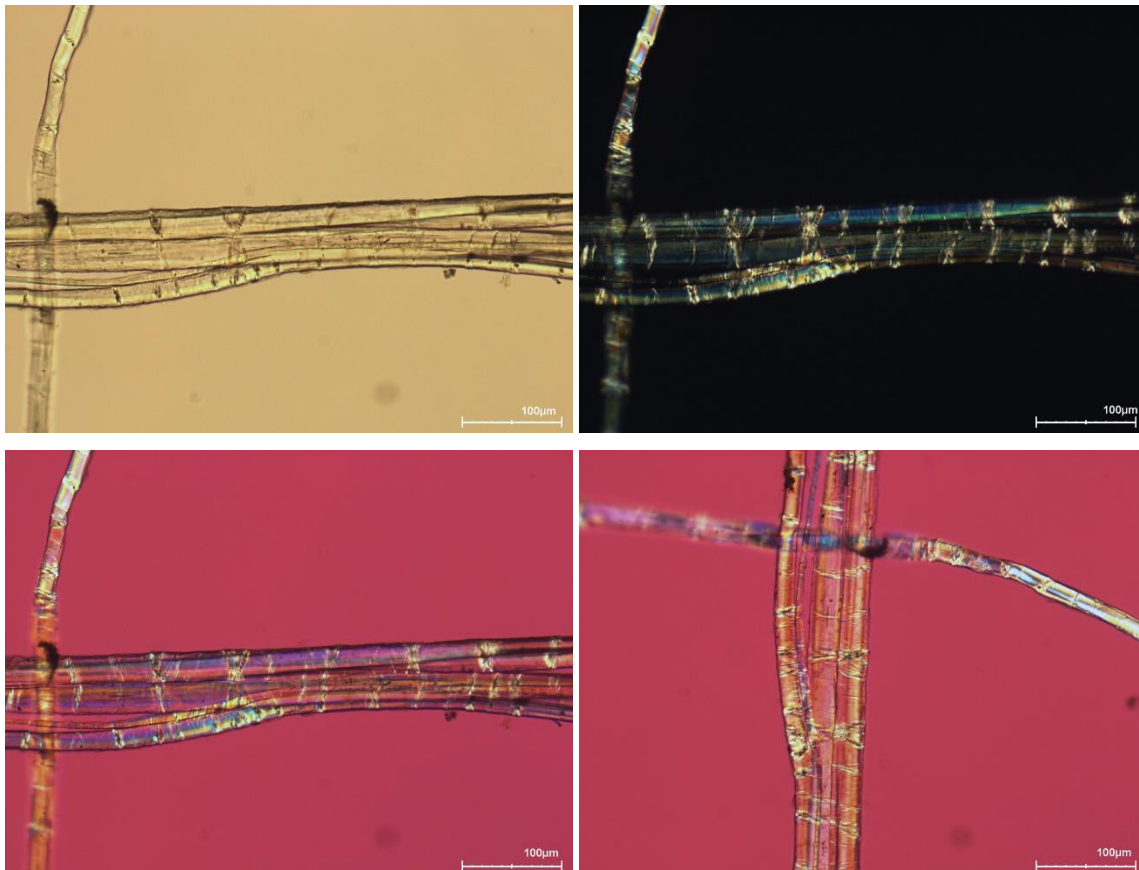


Figure 35: (top) microscopic images of sample 13621/m03 under transmitted light (left) and with the use of the polarisation filter (right) (magnification 200x); (bottom) red plate test images, the sample is blue in horizontal direction (left) and yellow in vertical direction (right) (magnification 200x)

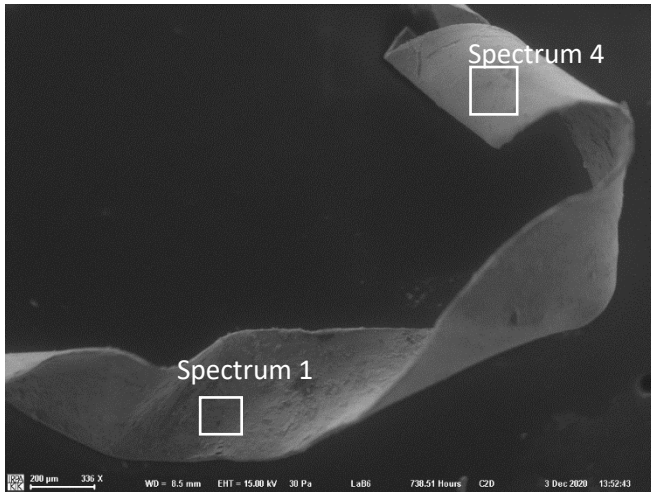


Figure 36: Secondary electron image of sample 13621/m03 with the indication of the analysed zones in white of the inside (spectrum 1) and the outside of the lamella (spectrum 4)

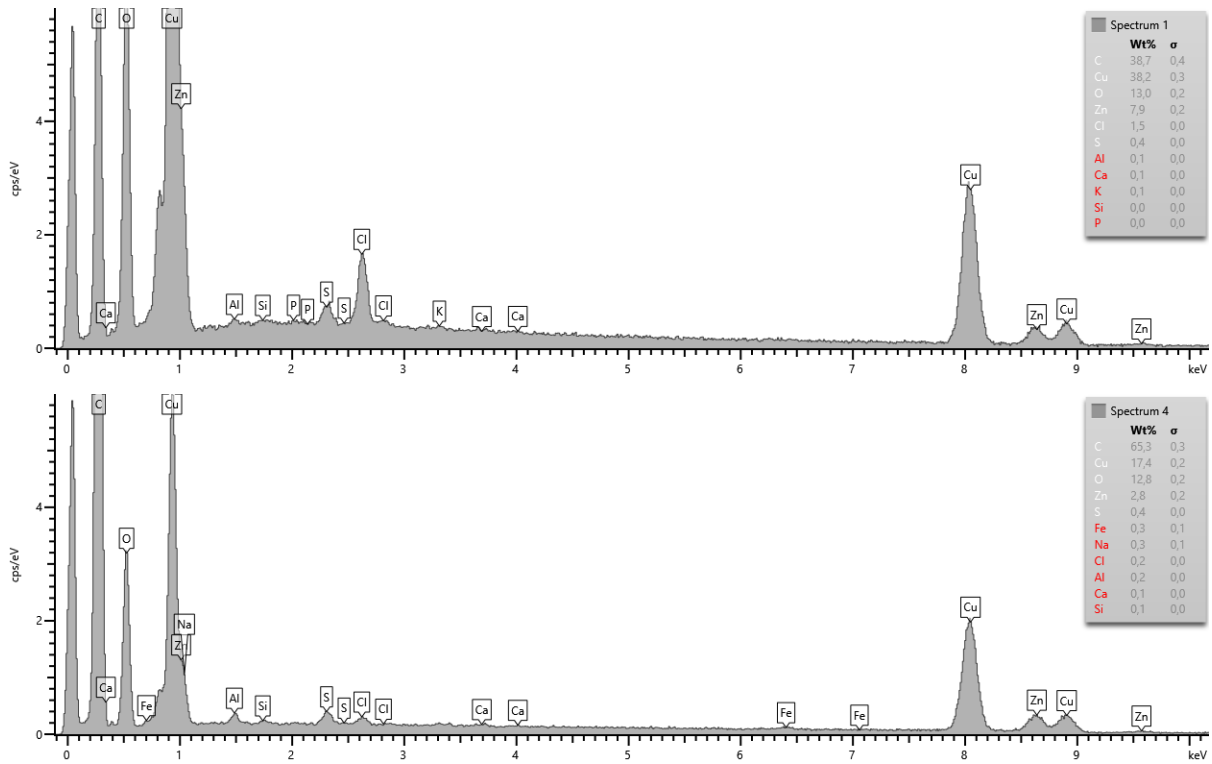


Figure 37: Element spectra of the inside (spectrum 1, top) and the outside of the metal lamella (spectrum 4, down) of sample 13621/m03

The SEM-EDX analysis of the metal lamella shows that the metal is also made of brass, an alloy of copper (Cu) and zinc (Zn) found in a relative ratio of 85/15 at the inside, and 83/17 at the outer surface (weight %). No traces of gold were found. The detection of chlorine (Cl) and sulfur (S), mainly on the inside, indicates the presence of corrosion of copper (figure 38-40).



Figure 38: Hirox image of sample 13621/m04 (magnification 40x)

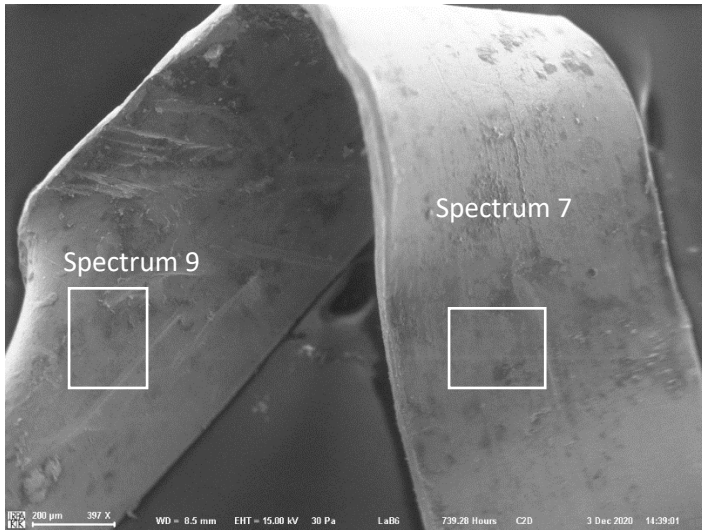


Figure 39: Secondary electron image of sample 13621/m04 with the indication of the analysed zones in white of the inside (spectrum 9) and the outside of the lamella (spectrum 7)

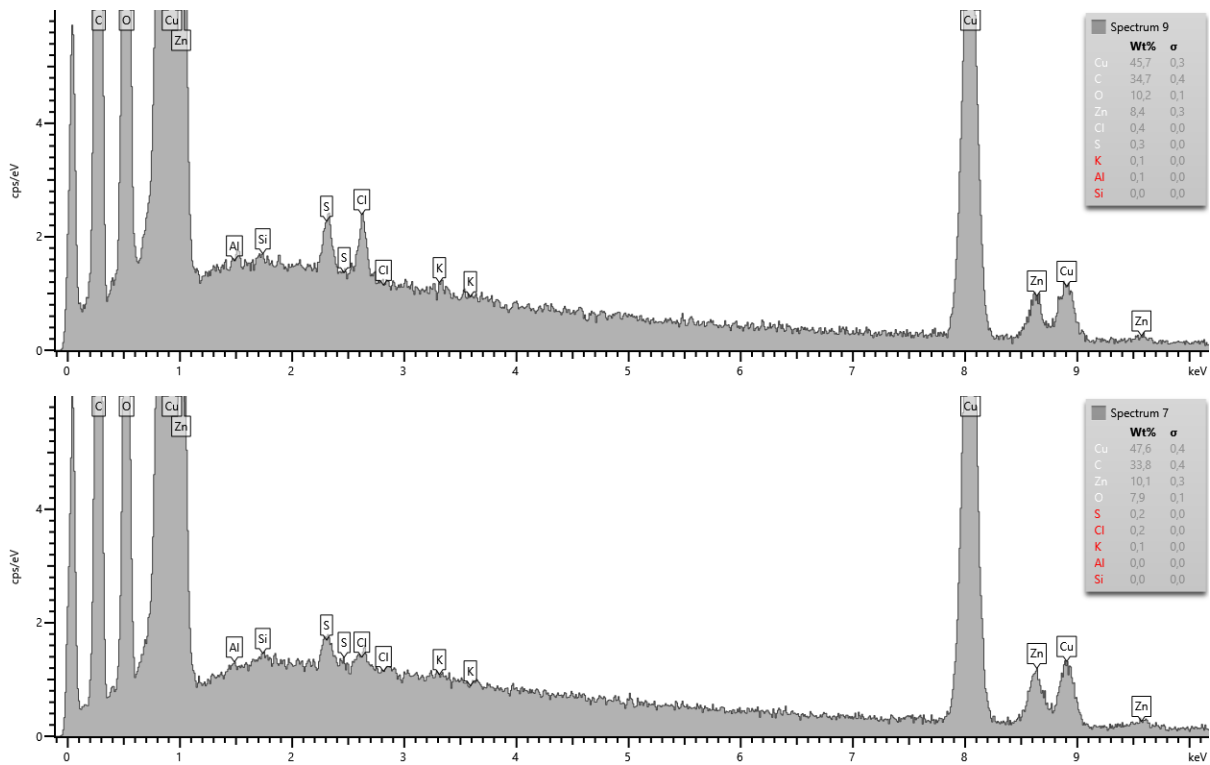


Figure 40: Element spectra of the inside (spectrum 9, top) and the outside of the lamella (spectrum 7, down) of sample 13621/m04

3. Conclusion

MA-XRF analysis of the decoration band at the border of the box unveils a different copper/zinc ratio for the wrapped thread and the flat lamella. This is also reflected in a color difference as shown by the Hirox images. This color difference (and hence a composition difference?) is not observed everywhere. The samples of both threads taken for SEM-EDX analysis showed a relative proportion (by weight) of 85 copper / 15 zinc for both threads. The metal thread with textile core is made of a metal strip wound in S-direction around a white textile core yarn. The fibres from that core yarn are identified as flax (*Linum usitatissimum* L.)

The MA-XRF identified as well the presence of brass nail heads and iron nails.

The red damask silk textile at the inside of the reliquary box has been dyed with Mexican cochineal (*Dactylopius coccus* species) and tannin. The dyeing of this textile completely matches that of a 'similar' fragment of red silk damask currently in the possession of the Diocesan Museum of Namén.

For the stuffing under the silk damask, flax fibres were used and not white horsehair (the more expensive and more prestigious alternative).

MA-XRF analysis of the enamel medallions on top of the box revealed that the metal support is a gilded copper plate with the gold applied by 'amalgam gilding'. Both the nails used to fix the copper plates onto the box and some of the nails used as circular decoration around the enamel medallions are composed of brass (in fact: not the nails themselves but the decorative rounded heads of the nails). Lead-tin alloy was used as solder material between the nail heads and the nails. This process was already described by Pliny the Elder 2000 years ago. All enamels contain cobalt(oxide) as blue colorant. Calcium antimonate and tin oxide are historically the most used opacifiers. The blue enamels on medallion 4, 6 and 9 contain antimony but no tin, these enamels could be dated as early 13th century.

The evenly distributed hair follicles showed that the original leather was made from cow or calf skins. The deterioration of this leather is probably a result of the combined effect of mechanical damage (nails used to fix the leather and thus perforating the leather) and damage by climatological conditions (large climatic variations make the leather shrink and expand causing deformations and cracks). The hair pores of the restoration leather are present in different clusters, spread out in wide-set rows. This points to a sheepskin. Part of the surface layer of this leather is already missing (deterioration of the leather).

4. References

(1967) Identification of Textile Materials. Published by the Textile Institute, Manchester, 5th edition

Cardon, D. (2007) Natural dyes. Sources, Tradition, Technology and Science, Archetype Publications, London, 619-631.

Haugan, E. and Holst, B. (2013) Determining the fibrillar orientation of bast fibres with polarized light microscopy: the modified Herzog test (red plate test) explained. *Journal of microscopy* 252 (2), 159-168.

Kshirsagar, S. V., Singh, B., Fulari, S. P. (2009) Comparative study of human and animal hair in relation with diameter and medullary index, *Indian Journal of forensic Medicine and Pathology* Vol.2 N°3, 105-108

Petraco, N. en Kubic, T. (2004) Colour atlas and manual of microscopy for criminalists, chemists and conservators, CRC press, 69-75

Vanden Berghe, I., Gleba, M. and Mannering, U. (2009) Towards the identification of dyestuffs in Early Iron Age Scandinavian peat bog textiles. *Journal of Archaeological Science* 36, 1910-1921

Vanden Berghe, I. (2016) The identification of Cochineal Species in Turkmen Weavings; A Special Challenge in the Field of Dye Analysis. In *Turkmen Carpets. A New Perspective*, volume I. Eds. Jürg Rageth and 'Freunde des Orientteppiche Basel', Abächerli Media AG, Sarnen (Switzerland), 303-310

Vanden Berghe, I., Vandorpe, M. and Coudray, A. (2020) KIK-IRPA (non-commercial) fibre reference database

Von Bergen, W. and Krauss, W. (1945) *Textile Fibre Atlas*, a collection of photomicrographs of old and new textile fibres. Textile book publisher Inc., New York (second printing)